ELSEVIER

Contents lists available at ScienceDirect

Biomaterials Advances

journal homepage: www.journals.elsevier.com/materials-science-and-engineering-c





Optimising a self-assembling peptide hydrogel as a Matrigel alternative for 3-dimensional mammary epithelial cell culture

Eliana Lingard ^{a,b}, Siyuan Dong ^c, Anna Hoyle ^{a,d}, Ellen Appleton ^{a,d,1}, Alis Hales ^{a,b}, Eldhose Skaria ^a, Craig Lawless ^a, Isobel Taylor-Hearn ^{a,b}, Simon Saadati ^{a,b}, Qixun Chu ^{c,f}, Aline F. Miller ^c, Marco Domingos ^e, Alberto Saiani ^{f,g}, Joe Swift ^{a,d}, Andrew P. Gilmore ^{a,b,*}

- ^a Wellcome Centre for Cell-Matrix Research, Oxford Road, Manchester M13 9PT, UK
- b Division of Cancer Sciences, School of Medical Sciences, Faculty of Biology, Medicine and Health, Manchester Academic Health Science Centre, University of Manchester, Manchester, M13 9PL, UK
- ^c School of Materials, Faculty of Science and Engineering, The University of Manchester, Oxford Road, Manchester, UK
- d Division of Cell Matrix Biology and Regenerative Medicine, School of Biological Sciences, Faculty of Biology, Medicine and Health, Manchester Academic Health Science Centre, University of Manchester, Manchester M13 9PL, UK
- e Department of Mechanical, Aerospace and Civil Engineering, School of Engineering, Faculty of Science and Engineering & Henry Royce Institute, The University of Manchester, United Kingdom, M13 9PL, UK
- f Manchester Institute of Biotechnology, University of Manchester, 131 Princess Street, Manchester, M1 7DN, UK
- g Division of Pharmacy and Optometry, School of Health Sciences, Faculty of Biology, Medicine and Health, University of Manchester, Manchester M13 9PL, UK

ARTICLE INFO

Keywords: Hyrodgels Breast epithelial cells Breast cancer Matrigel Laminin Mammary differentiation

ABSTRACT

Three-dimensional (3D) organoid models have been instrumental in understanding molecular mechanisms responsible for many cellular processes and diseases. However, established organic biomaterial scaffolds used for 3D hydrogel cultures, such as Matrigel, are biochemically complex and display significant batch variability, limiting reproducibility in experiments. Recently, there has been significant progress in the development of synthetic hydrogels for in vitro cell culture that are reproducible, mechanically tuneable, and biocompatible. Self-assembling peptide hydrogels (SAPHs) are synthetic biomaterials that can be engineered to be compatible with 3D cell culture. Here we investigate the ability of PeptiGel® SAPHs to model the mammary epithelial cell (MEC) microenvironment in vitro. The positively charged PeptiGel® Alpha4 supported MEC viability, but did not promote formation of polarised acini. Modifying the stiffness of PeptiGel® Alpha4 stimulated changes in MEC viability and changes in protein expression associated with altered MEC function, but did not fully recapitulate the morphologies of MECs grown in Matrigel. To supply the appropriate biochemical signals for MEC organoids, we supplemented PeptiGels® with laminin. Laminin was found to require negatively charged PeptiGel® Alpha7 for functionality, but was then able to provide appropriate signals for correct MEC polarisation and expression of characteristic proteins. Thus, optimisation of SAPH composition and mechanics allows tuning to support tissue-specific organoids.

1. Introduction

The mammary gland undergoes dramatic changes during puberty, the menstrual cycle, pregnancy, lactation and involution. These changes involve complex molecular remodelling events involving cells and their extracellular matrix (ECM), dysregulation of which is implicated in breast cancer [1,2]. Many of the molecular networks regulating

mammary gland development, remodelling and cancer are poorly defined. One important approach to study these processes is through in vitro organoid models, which combine some of the strengths of two-dimensional (2D) culture systems with in vivo systems [3]. An organoid model needs to mimic the key features of the tissue in question, although there are often limitations in how well this can be achieved [4]. Consequently, there is a significant need to develop materials that better

^{*} Corresponding author at: Wellcome Centre for Cell-Matrix Research, Faculty of Biology, Medicine and Health, A.3034 Michael Smith Building, University of Manchester, Oxford Road, Manchester M13 9PT, UK.

E-mail address: andrew.gilmore@manchester.ac.uk (A.P. Gilmore).

 $^{^{\}rm 1}$ Present address: Department of Clinical Neuroscience, Karolinska Institutet, Stockholm, Sweden.

recapitulate the biochemical and biomechanical properties of a tissue while being experimentally reproducible. It is also valuable to be able to independently manipulate the properties of a synthetic tissue in order to understand their function. The development of novel biomaterials has been a key to the improvement of tissue-specific models [5].

Mammary gland organoid models have largely relied on a reconstituted basement membrane (BM) extract, Matrigel [6]. First described in 1977 as a rich source of BM proteins [7], Matrigel was subsequently used as a hydrogel for three-dimensional (3D) mammary epithelial cell (MEC) cultures, promoting them to form polarised acini that recapitulated aspects of in vivo function [8]. Matrigel is derived from the Engelbreth-Holm-Swarm (EHS) mouse sarcoma and is enriched in ECM components like collagen-IV, laminin, entactin and perlecan [7]. These allow Matrigel to support MEC differentiation into organoids that produce milk proteins in response to prolactin [9]. Matrigel also contains numerous growth factors and cytokines which contribute to the behaviour of embedded cells [6]. This broad functionality and bioactivity mean it remains popular for 3D organoid cultures.

Matrigel and similar tumour-derived materials suffer from limitations as an organoid scaffold [6]. Matrigel is biochemically complex, containing approximately 1800 proteins identifiable by mass spectrometry [10]. These include various growth factors and cytokines capable of affecting cell behaviour [11]. This complexity is exacerbated by variations between different production batches, both in total protein concentration and specific composition, resulting in inconsistency across experiments [6]. Matrigel contains tumorigenic factors that may stimulate pro-oncogenic cell behaviours, a potential issue for modelling non-tumorigenic tissue environments [12]. Matrigel's mechanical properties also suffer from batch-to-batch variation, affecting cell behaviour independently from its composition [13,14]. Matrigel is mechanically weak, and its mechanical properties are difficult to modify due to the interplay between matrix density and pore size with matrix stiffness. Finally, Matrigel is xenogenic and unrepresentative of human tissues, which introduces the risk of exposing cells to contaminants such as the immunogenic lactate dehydrogenase-elevating virus (LDV) [15].

The limitations of Matrigel have prompted development of cell scaffolds that offer more consistency, definition and tuneability. Synthetic polymers such as polyethylene-glycol (PEG) or polyacrylamide (PAM) are widely used. Their simple composition and flexible crosslinking chemistries make them amenable to specific cell culture applications [16]. Monomeric acrylamide is cytotoxic, making it incompatible for embedding cells for 3D culture, but PEG hydrogels have been successfully functionalised with ECM mimetic peptide motifs for 3D MEC culture [17].

Self-assembling peptide hydrogels (SAPHs) are a class of promising synthetic scaffolds for 3D culture. SAPHs are short, synthetic, amphipathic peptides that self-assemble into fibrillar structures. These fibres entangle with each other in water to form hydrated, fibrillar scaffolds [18]. SAPHs are simple, well defined and reproducible, making them amenable to a variety of modifications [19,20]. Furthermore, being peptide-based, SAPHs are inherently biocompatible. Different peptide sequences allow for variation in hydrogel properties such as charge and stiffness, allowing properties to be selected for specific applications [18]. Indeed, multiple studies have demonstrated that 3D SAPHs are capable of supporting the development of tissue organoids [21-24]. In one study SAPH-encapsulated human induced pluripotent stem cells (hiHSCs) organised into heterogenous kidney organoids which were viable for at least 24 days and produced their own basement membrane [25]. Here we investigate the potential for beta-sheet forming SAPH PeptiGels® to model MEC function in vitro. Both positively charged PeptiGel® Alpha4 ("Alpha4") and negatively charged PeptiGel® Alpha7 ("Alpha7") support MEC viability and proliferation. However, both Alpha4 and Alpha7 have limited bioactivity and were unable to promote complex MEC acinar morphogenesis. We investigated whether modifying SAPH properties through altering their mechanical stiffness and functionalising them with laminin-111 to form a hybrid hydrogel

promoted MEC function. We found that the combination of laminin and negatively charged Alpha7 enabled MEC-specific protein expression and acinar morphology.

2. Materials and methods

2.1. Cell culture

Immortalised, non-tumorigenic human mammary epithelial cells (MCF10A) were sourced from ATCC and maintained in DMEM-F12 media supplemented with 5 % filtered horse serum, 10 µg/mL insulin, 0.5 µg/mL hydrocortisone, 100 ng/mL cholera toxin and 20 ng/mL EGF. Cells were passaged at 70–90 % confluency.

PeptiGels® were purchased from Manchester BIOGEL (Alderley Park, UK) and are now sold by Cell Guidance Systems (Cambridge, UK). Matrigel and collagen I were purchased from Corning Life Sciences. High-concentration Cultrex 3-D Culture Matrix laminin-I was purchased from Trevigen.

For encapsulation of MCF10A cells into 3D gels, wells of a 24-well plate were coated with a 50 μL layer of either undiluted Matrigel (8.9 mg/mL) or high-concentration laminin-I (6.1 mg/mL) and left to set for 30 min at 37 °C. Passaged MCF10A cells were resuspended in 1 mL of media. For Matrigel, cell suspensions were mixed into blank DMEM to give a volume of 49.5 μL per gel, and 50.6 μL of 8.9 mg/mL Matrigel was added to give a final total protein concentration of 4.5 mg/mL and cell density of 0.5 \times 10 5 cells per 100 μL of gel. 100 μL of the Matrigel-cell-DMEM solution was then added to each well before polymerising at 37 °C/5 % CO2 for 30 min. For laminin I gels, MCF10a cells in culture media were mixed with 6.1 mg/mL laminin-111 to a final concentration of 5.49 mg/mL and a cell density of 0.5 \times 10 5 cells per 100 μL of gel. 100 μL of laminin-cell mixture was then pipetted into each well and left to polymerise at 37 °C (5 % CO2) for 30 min. The gels were bathed in media which was refreshed every 2–4 days.

For collagen gels, collagen-I at a final concentration of 1.5 mg/mL (prepared from 3.98 mg/mL collagen I, 104 μL DMEM and 20 μL $10\times$ Roswell Park Memorial Institute (RPMI) media, neutralised by adding 3 μL of 1 M sodium hydroxide) was spread over the bottom surfaces of 24-well plates and left to set for 30 min at 37 °C/5 % CO_2. MCF10A cells were prepared in 200 μL 1.5 mg/mL collagen-I prepared as above. The gels were incubated for 30 min and bathed in media which was refreshed every 2–4 days.

For SAPH cultures, 50 μL of PeptiGel® at room temperature was spread over the bottom surface of wells in 24-well plates. MCF10A cells were encapsulated via gentle pipetting into appropriate volumes of SAPH, with a final cell density of 0.5×10^5 cells per mL. Following encapsulation, 100 μL of cell-laden hydrogels were pipetted into each well on top of the gel layer. Culture media was added and refreshed every 2–4 days.

To isolate intact organoids for either re-encapsulation in hydrogels or for immunofluorescent staining, 3D cultures were washed with 1 mL of PBS following removal of media and then depolymerised using 1 mL of ice-cold cell recovery solution (Corning) for 1 h at 4 °C. The depolymerised gels were resuspended, collected into tubes pre-coated with 1 % BSA in PBS (w/v) and washed via centrifugation in PBS at 70 RCF. The supernatants were discarded, and the organoid pellets resuspended for re-encapsulation or fixed for staining.

2.2. Oscillatory shear rheometry

The storage modulus of gels was measured using a Discovery HR-2 hybrid rheometer (TA Instruments, USA) with a 20 mm (mm) parallel plate and a gap size of 500 μM . Samples were prepared by aliquoting 180 μL of gel into ThinCert well inserts (1 μM pore size, Greiner Bio-One Ltd., Gloucestershire, UK). 900 μL of assay media was pipetted into the wells after 5 min and left to recover for 5 min before 100 μL of media was added to each insert. The gels were incubated at 37 °C (5 % CO₂) for at

least 30 min prior to testing. Following media exposure, samples were removed from the inserts by peeling off the bottom membrane of the insert and transferred onto the rheometer plate as described by Ligorio et al. [4]. The upper rheometer head was then lowered to the gap size and samples were equilibrated for 3 min at 37 $^{\circ}$ C. Oscillatory amplitude experiments were performed at 1 Hz frequency and within the linear viscoelastic region in the strain range: 0.01 to 20 %. The mean storage modulus values described in the results section were obtained at 0.2 % oscillation strain. All measurements were repeated three times to ensure reproducibility.

2.3. Immunofluorescent staining and microscopy

Extracted MCF10A organoids were fixed for 45 min in 4 % formaldehyde in PBS (ν/ν) at room temperature, diluted with 10 mL of PBS and centrifuged at 70 RCF for 3 min at 4 $^{\circ}$ C. The pellets were resuspended in 1 mL of organoid wash buffer (PBS containing 0.1 % Triton-X-100 and 0.2 % BSA), transferred to pre-coated, low adherent 24-well plates (Greiner Bio-One) and blocked for 15 min. Cell clusters were incubated with 2× primary antibodies in organoid wash buffer overnight at 4 °C. The plates were retrieved, washed three times in organoid wash buffer for 1 h at 4 °C. Clusters were incubated with 2× secondary antibody solutions in organoid wash buffer overnight at 4 °C, incubated with 2 µg/mL DAPI in PBS for 10 min on an orbital shaker before being washed 3 times with organoid wash buffers as described above. Organoids were diluted in PBS and transferred to 6-well plates for imaging. Confocal images were collected on a Leica TCS SP8 AOBS upright confocal using a 63×/0.90 water immersion objective. The confocal settings were as follows, pinhole 1 airy unit, scan speed 400 Hz unidirectional, format 1024×1024 . Images were collected using hybrid and photomultiplier detectors with the following detection mirror settings; DAPI 410-475 nm; Alexa-488,507-580 nm; Alexa-594,605-750 nm using the 405 nm (50 %), 490 nm (30 %) and 590 nm (30 %) laser lines respectively. When it was not possible to eliminate crosstalk between channels, the images were collected sequentially. The acquired images were processed using ImageJ.

Primary antibodies used for immunofluorescent staining were: active caspase-3 (Rabbit, R&D Systems, AF835); human laminin alpha3 chain (Mouse, R&D Systems, MAB21441); native collagen IV (Rabbit, Abcam, ab6586); β -catenin (Mouse, BD Biosciences, 610,154). Secondary antibodies were from Invitrogen (donkey anti-mouse AlexaFluor 594, A21203; donkey anti-rabbit AlexaFluor 488 A21206).

2.4. Assessment of MCF10A cell clusters

To assess organoid size and density, encapsulated MCF10A organoid hydrogels were prepared in triplicate as above and cultured for up to 21 days and fixed on either day 7, 14 or 21 as above. Fixed clusters were then stained with 1 $\mu g/mL$ DAPI in PBS for 10 min, washed with 3D IF wash buffer for 10 min and then double-distilled water overnight. Fluorescent images of DAPI-stained clusters were collected as Z-stacks on an EVOS M7000 Imaging system (Thermo Fisher Scientific) using a $4\times$ PlanFL 0.13 NA objective using the DAPI light cube. The acquired images were processed in QuPath 0.2.3 by manually counting fluorescent nuclei. Measurements were exported to GraphPad Prism for statistical analysis.

Clusters formed in Matrigel and laminin-111 were analysed in ImageJ to assess their area and circularity. Clusters in focus were traced around their periphery using the freehand tool (to measure circularity) or the freehand line tool (to measure area). The tracing was done by hand using a Wacom One drawing tablet and pen. Measurements were exported to GraphPad Prism.

To quantify BM organisation, acinar volume was approximated by combining the nuclear and membrane fluorescence intensity images and clipping to reduce the dynamic range. A Gaussian filter was used to smooth the images and a mean threshold was applied to segment the

binary image. Holes and small objects were removed. Morphological erosion was used to distinguish individual acini, especially when they were merely proximal or superficially connected rather than genuinely forming a single, non-spherical entity. A distance transform was used to calculate the shortest Euclidean distance between each point on the identified acinus and its boundary. Laminin intensity outside the identified acinar region was set to 0, to avoid inclusion of laminin from adjacent acini in the analysis. The average laminin intensity at each distance from the acinus exterior was calculated. Distance from the acinus exterior and average intensity were both normalised between 0 and 1 for each acinus. Well-polarised acini should display a sharp intensity peak at the exterior, rapidly diminishing toward the centre. A less uniform phenotype will result in a flatter average laminin intensity distribution.

2.5. Mass spectrometry analysis

Hydrogel-encapsulated MCF10A cell organoids were lysed in 100 μL of $1\times\,$ radioimmunoprecipitation (RIPA) buffer (50 mM Tris-HCL/pH 7.4, 150 mM sodium chloride, 1 % IGEPAL, 0.1 % (w/v) SDS, 1 % sodium deoxycholate, 20 mM sodium fluoride, 2 mM sodium orthovanadate, $1\times\,$ protease inhibitor cocktail). Following 15 min incubation on ice, the samples were sonicated for 180 s using a Covaris S220 ultrasonicator before being centrifuged at 3220 xg for 5 min at 4 °C. Lysates were stored at 20 °C prior to use.

Lysates were prepared for mass spectrometry using SDS-PAGE electrophoresis. Samples were allowed to migrate past the wells of a pre-cast 4–20 % polyacrylamide gel. Once stained with InstantBlue, gel sections were submitted for peptide identification analysis to the University of Manchester Biological Mass Spectrometry Core Facility. The samples underwent in-gel digestion before being analysed using the Thermo Orbitrap Elite mass spectrometer coupled with a Thermo nanoRSLC system.

Raw data files were processed in MaxQuant (v 2.0.1.0) [26]. Spectra were searched against the Human (Homo Sapiens) reference proteome obtained from Uniprot (June 2021), which was modified to include the three murine laminin I subunit (LAMA1_MOUSE, LAMB1_MOUSE, LAMC1_MOUSE) peptide sequences obtained from the Mouse (Mus musculus) reference proteome (July 2021) [27]. Methionine oxidation and N-terminal acetylation were set as variable modifications and cysteine carbamidomethylation was set as a fixed modification. Fast label-free quantification was enabled, with a minimum label ratio of 2 selected. A minimum of 3 and an average of six sample neighbours were also set. Precursor tolerance for the first and main searches was set at 20 ppm and 4.5 ppm, respectively. MS/MS tolerance was set at 20 ppm, with a maximum of two missed cleavages allowed. The false discovery rate (FDR) of PSM and protein were set at 0.01 and "Match between runs" was enabled. MaxQuant peptides.txt and proteinGroups.txt output files were processed in R (v 4.1.2). Contrasts were set up and run using MsqRob2 (v 1.2.0) [28], where only proteins of FDR <0.05 were considered significant.

Gene ontology enrichment analysis was performed using the cluster Profiler package (v 4.0) [29]. Separate lists of significantly upregulated and downregulated ENTREZID gene IDs were queried against the org. Hs.eg.db (v 3.14.0) database. Overrepresentation analysis was performed and corrected for FDR using the Benjamani-Hochberg method by cluster Profiler to determine enriched genes in the lists. Only genes of $p \leq 0.05$ were considered significant. Pathway enrichment analysis was then performed using Reactome PA (v1.38.0) [30], where separate lists of significantly upregulated and downregulated ENTREZID gene IDs were queried against the org. Hs.eg.db database and subject to overrepresentation analysis using the Benjamani-Hochberg method to determine enriched pathways and interaction networks. Only genes of p ≤ 0.05 were considered significant. All enriched genes and pathways were visualised in R using enrichplot (v 1.14.1).

2.6. Statistical analysis

All quantitative values are presented as mean \pm standard deviation unless stated otherwise in the text. Data was analysed using one-way or

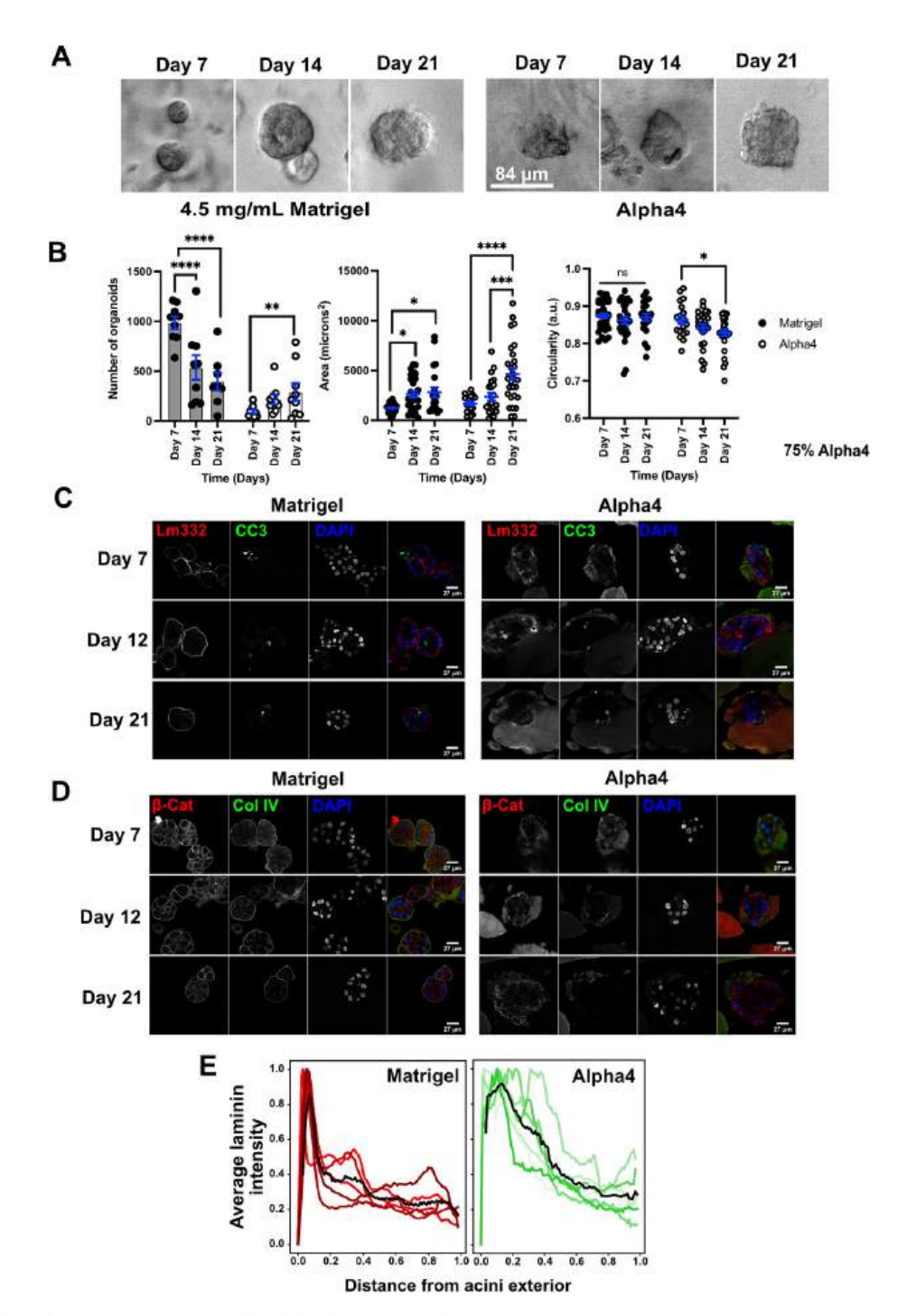


Fig. 1. PeptiGel® Alpha4 alone supports MCF10A cell viability but does not allow 3D acinar organisation.

A. Representative brightfield images of MCF10A cells encapsulated in Matrigel and Alpha4 (scale bars, $84 \mu m$). MCF10A MECs were encapsulated into Matrigel or PeptiGel® Alpha4 for 7, 12 or 21 days.

B. Comparison of organoid number, size and circularity between MCF10A cells embedded in Matrigel or Alpha4 for 7, 14 and 21 days. Experiments were repeated at least 3 times and data are shown as mean \pm SEM (* *P*-value <0.05, ** *p*-value <0.01, *** *p*-value <0.001, *** *p*-value <0.0001)

C. MCF10A cell organoids were grown in either Matrigel or Alpha4 for the indicated number of days. Organoids were extracted from the 3D cultures and immunostained for human laminin-332 (Lm332) and cleaved caspase-3 (CC3). Nuclei were stained with DAPI (scale bars, 27 µm).

D. MCF10A organoids as in C were immunostained for β -catenin (β -Cat) and collagen-IV (Col IV). Nuclei were stained with DAPI (scale bars, 27 μ m).

E. Quantitation of laminin-332 organisation relative to acinar volume for MCF10A organoids in either Matrigel or Alpha4 at Day 12 of culture. The average laminin intensity at each distance from the acini exterior was calculated. Distance from the acinus exterior and average intensity were both normalised between 0 and 1 for each acini. Five individual acini were analysed for each condition, the black line represents the mean. Well-polarised acini show a sharp intensity peak at the exterior.

3. Results

3.1. Alpha4 supports MEC viability but not acinar polarisation of MCF10A cells

Alpha4 is a positively charged SAPH that has previously been shown to maintain viable cultures of mouse MECs for up to 7 days [27]. It has also been shown to support cultures of human mesenchymal stem cells and rabbit synoviocytes [21,23]. We therefore first assessed the ability of Alpha4 as a cell culture scaffold for the human, non-malignant mammary epithelial cell line MCF10A. MCF10A cells are a wellestablished model for normal mammary organoid development and polarity, and their behaviour within 3D Matrigel is well characterised [31]. We encapsulated MCF10A cells in either Alpha4 or Matrigel, and allowed them to grow over 21 days, during which time we monitored viability, acinar size and morphology. Cells were viable in Alpha4 for at least 21 days, as shown by brightfield microscopy, and formed clusters that superficially resembled the 3D acinar structures formed in Matrigel (Fig. 1A). We compared clusters grown in Alpha4 and Matrigel and measured their number, size and circularity (Fig. 1B). 3D cultures were stained with DAPI at days 7, 14 and 21, and fluorescent images taken for image analysis. The number of acinar structures observed in Matrigel declined over 21 days, with 987 \pm 187 (+/- SEM) organoids counted at day 7 compared to 397 \pm 255 organoids counted in Matrigel on day 21 (Fig. 1B). In contrast, the number of cell clusters in Alpha4 increased over 21 days from 96 \pm 55 (+/- SEM) clusters at day 7 to 291 \pm 267 clusters at day 21. We compared the morphology of organoids grown in Alpha4 and Matrigel at days 7, 14 and 21 by measuring their area and circularity. In Matrigel, MCF10A acini undergo growth arrest after around 14 days, with measurable cross-sectional areas between 1000 and 9000 µm² (Fig. 1B). This acinar growth arrest has been previously shown to correspond with reduced cell proliferation [31,32]. However, cell clusters in Alpha4 continued to grow, and were significantly larger than those in Matrigel at day 21. Clusters in Alpha4 also had significantly lower circularity compared to Matrigel, suggesting poorer acinar organisation (Fig. 1B).

To compare organisation of the 3D cell clusters in Matrigel and Alpha4, we examined localisation and expression of key markers of MCF10A organoid formation. Intact cell clusters were extracted from Matrigel or Alpha4 at days 7, 12 and 21, and fixed in paraformaldehyde. These were immunostained with antibodies against human specific laminin-alpha 3 (alpha chain of laminin-332), collagen-IV (recognises only native forms of both mouse and human col. IV), the cell-cell junction marker β-catenin, and cleaved caspase-3, a marker of apoptosis that occurs in the inner cells of MCF10A acini in Matrigel (Fig. 1C and D). In Matrigel, MCF10A cells had a clearly defined BM surrounding the acini, containing human laminin and collagen-IV. In contrast, cell clusters from Alpha4 lacked an organised collagen-IV and laminin-332 BM, despite both proteins appearing to be present. We quantified the ability of MCF10A cells in either Matrigel or Alpha4 to organise a basement membrane by carrying out segmentation analysis of confocal images of laminin immunofluorescence (Fig. 1E). There was a clearly defined peak identified in acini grown in Matrigel at 12 days corresponding to the acinar edge. In contrast, acini in Alpha4 show more variability and no clear peak of BM at the acini edge. Importantly, although Matrigel contains murine collagen IV, immunostaining clearly shows organised, native collagen IV only around the MCF10A acini in Matrigel. Cleaved caspase-3 was seen in cells within the Matrigel acini, and β-catenin indicated cell-cell adherens junctions. In Alpha4 caspase-3 activity was broadly distributed, and β -catenin was seen, indicating cellcell adherens junctions.

Overall, these data revealed that although Alpha4 supports MCF10A viability, it is unable to fully recapitulate the MCF10A organisation seen in Matrigel.

3.2. The mechanical properties of Alpha4 hydrogels can be tuned by dilution

ECM stiffness has been shown to affect a range of cellular behaviours, including regulation of gene expression and differentiation [33,34]. We therefore asked whether the inability of Alpha4 to fully recapitulate MCF10A behaviour in Matrigel was due to differences in the stiffness of the two materials. We performed oscillatory shear rheometry on Alpha4 and 4.5 mg/mL Matrigel, using amplitude sweep analysis on three independent preparations of each gel. Gels were preconditioned in culture media at 37 $^{\circ}$ C and 5 % CO₂. Each preparation was measured three times at 1 Hz frequency within the linear viscoelastic region in the strain range 0.01 to 20 % (Fig. 2A). Alpha4 showed a storage modulus (G') of \sim 400 Pa, although other data have also reported it to be in the region of 650 Pa [25]. In marked contrast, 4.5 mg/mL Matrigel had a G' of ~6 Pa. Published rheology data on Matrigel has reported widely different values of G' that can be up to 5-fold stiffer, but also within the range measured here, possibly reflecting variations in batches and methodology [14,35]. However, Matrigel is considerably softer than Alpha4.

We considered the possibility that the stiffness of Alpha4 prevented MCF10A differentiation. Several studies have modified the stiffness of Matrigel to better mimic tissue mechanics. One way to achieve this is with an interpenetrating network of Matrigel and the polysaccharide alginate, which can be crosslinked with calcium ions to stiffen the network [14]. Matrigel-alginate gels with 2.4 mM and 20 mM CaSO₄ have reported G' values of around 80 and 310 Pa respectively, compared with 30 Pa without crosslinking [14]. Since Alpha4 is a porous network of peptides and water, we hypothesised that we could reduce the G' by diluting it with phosphate-buffered saline (PBS). We found that Alpha4 could be diluted by up to 50 % before the hydrogel began to fragment. This dilution limit was probably because the peptide network became unable to accommodate additional fluid. Amplitude sweeps showed that diluting Alpha4 with up to 50 % (ν/ν) PBS reduced its G' to \sim 150 Pa (Fig. 2B). Thus, Alpha4 can be reproducibly modified by dilution to create softer gels.

We compared these values for Alpha4 with Matrigel-alginate hydrogels. We performed rheology on soft (0 mM CaSO₄), medium (2.4 mM CaSO₄), and stiff (20 mM CaSO₄) Matrigel-alginate gels at 1 Hz frequency (Fig. 2C). Matrigel-alginate hydrogels displayed elastic behaviour across the strain range 0.01–20 % and increased in stiffness with CaSO₄ addition. Soft Matrigel-alginate gels had a mean value of G' of 4.2 Pa, similar to Matrigel alone. 2.4 mM CaSO₄ increased mean G' to 9.2 Pa. The stiffest Matrigel-alginate gels, with 20 mM CaSO₄, showed a mean G' of 171.8 Pa. As with Matrigel alone, these values are almost 5-fold lower than published measurements with similar Matrigel-alginate hydrogels. These data suggest that making direct comparisons between independent studies is difficult. However, diluting the SAPH Alpha4 (with PBS) brought its G' value into the range achievable with Matrigel.

3.3. Softening the Alpha4 hydrogel by dilution is insufficient to cause acinar polarisation of MCF10A cells

We next examined the behaviour of MCF10A cells encapsulated in soft (50 % ν/ν) and medium (75 % ν/ν) Alpha4 hydrogels. Single MCF10A cells were encapsulated in each gel and grown for 7, 12 and 21 days (Fig. 2D). Cell clusters were then isolated, fixed and immunostained as before (Fig. 2E). Diluting Alpha4 did not improve the organisation of MCF10A acini. Localisation of laminin and collagen-IV both showed a similar distribution to that observed with cells grown in undiluted Alpha4. Although both ECM proteins did appear to be secreted, they were not organised into the defined BM seen with cells cultured in Matrigel, confirmed by segmentation analysis (cf. Fig. 1C, D and E). β -catenin and cleaved caspase-3 also showed a distribution similar to that in undiluted Alpha4. We quantified the number, size, and circularity of MCF10A clusters in 75 % and 50 % Alpha4 hydrogels. Reducing the stiffness of Alpha4 appeared to encourage increased cluster viability,

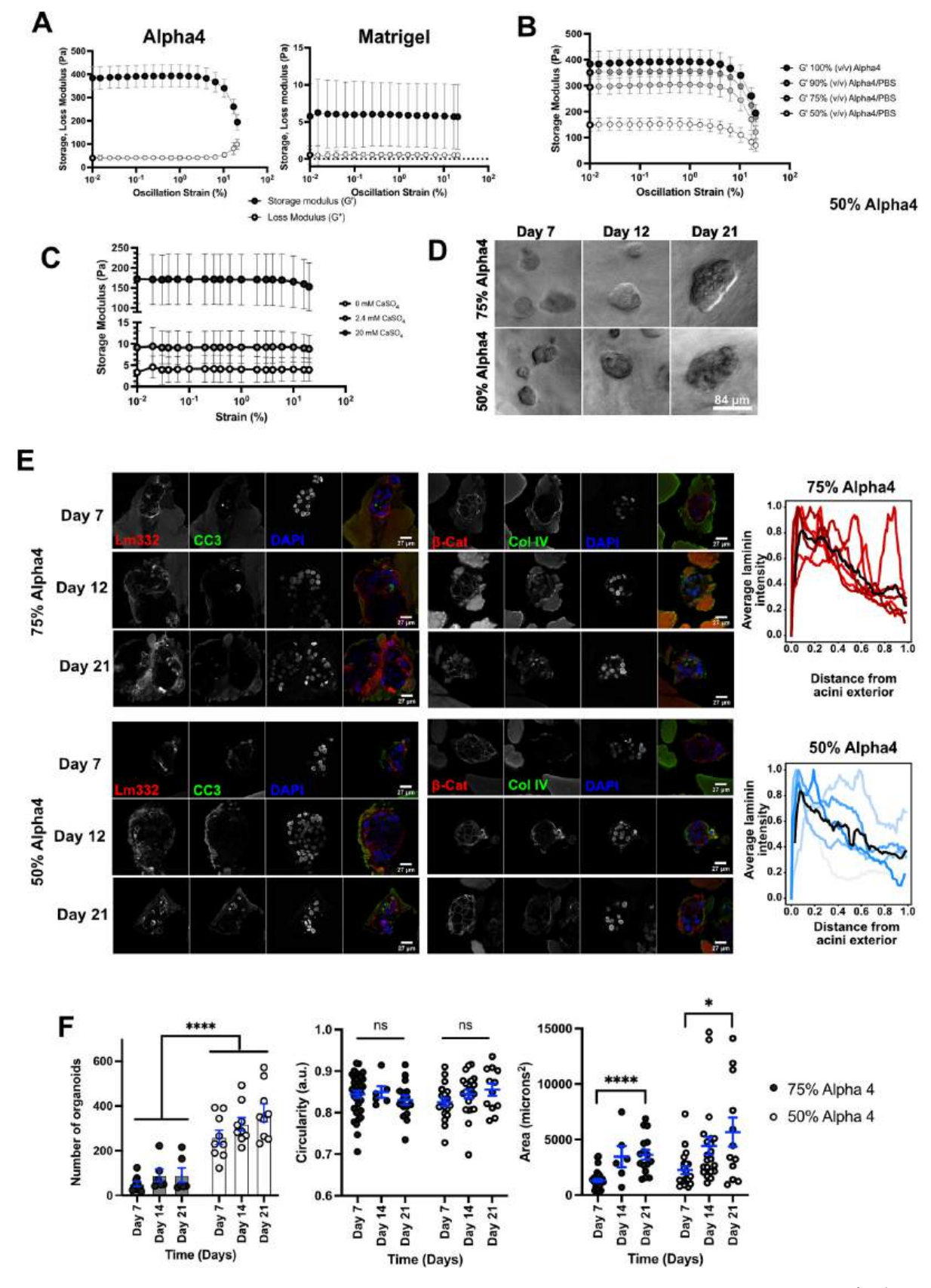


Fig. 2. Modifying Alpha4 hydrogels stiffness increases organoid viability but does not alter their polarity.

A. Oscillatory rheometry comparison of storage (G') and loss modulus (G") between Alpha4 and 4.5 mg/mL Matrigel. Measurements were taken at 1 Hz. All measurements were performed at least 3 times. Means \pm SD are shown.

B. Storage moduli at 1 Hz of PeptiGel® Alpha4 diluted with different volumes of PBS to the indicated proportions. All measurements were performed at least 3 times. Means \pm SD are shown.

C. Storage moduli at 1 Hz of Matrigel-alginate hydrogels stiffened using the indicated concentrations of calcium sulphate $(CaSO_4)$. Means \pm SD are shown. All measurements were performed at least 3 times, but underloading of some Matrigel-alginate samples at 20 mM CaSO₄ led to their exclusion from analysis.

D. MCF10A organoid viability assessed in diluted Alpha4. Representative brightfield images of MCF10A cells encapsulated in 50 % and 75 % Alpha4 gels over 7, 12 and 21 days (scale bars, 84 μ m).

E. MCF10A cells were cultured within Alpha4 hydrogels at either 75 % or 50 % for 7, 12 or 21 days before organoids were isolated and immunostained for human laminin- α 3 (Lm332), cleaved caspase-3 (CC3), β-catenin (b-Cat) and collagen-IV (Col IV), as indicated. Nuclei were stained with DAPI (scale bars, 27 μm). For the Day 12 images, laminin-332 organisation relative to acinar volume was quantified, showing the average laminin intensity at each distance from the acini exterior as in Fig. 1E. Coloured lines show individual acini, and the black line the mean.

F. Comparison of organoid number, size and circularity between MCF10A cells embedded in 75 % or 50 % Alpha4 hydrogels for 7, 12 and 21 days. All measurements were performed at least 3 times. Data are shown as mean \pm SD. P-values: * <0.05; ** <0.01; *** <0.001; **** <0.0001.

in both the medium and soft gels compared to stiff Alpha4 (cf. Fig. 2E and Fig. 1B). Although we saw no differences in the circularity of cell clusters between any of the Alpha4 hydrogel preparations (Fig. 2F), they did grow into larger organoids when the SAPH was softer.

To gain a holistic view of how softening the SAPH altered MCF10A cell function, and how this compared with cells cultured in Matrigel, we performed mass spectrometry (MS) analysis comparing acini grown in 75 % and 50 % Alpha4 with cells grown in 4.5 mg/mL Matrigel. MCF10A cells were encapsulated into each hydrogel and grown for 14 days, after which clusters were extracted and processed for liquid chromatography coupled tandem MS (LC-MS/MS). To exclude exogenous proteins originating from the media or hydrogel from the downstream comparison, we also analysed samples of cell-free Alpha4 and Matrigel. Approximately 800-1000 unique proteins were identified in each sample. Principal component analysis (Fig. 3A) indicated clear separation between all three conditions with encapsulated cells, with the most separation observed between cells in Matrigel and those in either 75 % or 50 % Alpha4. However, there was separation between the two Alpha4 conditions, indicating that altering the mechanical stiffness of the SAPH altered MCF10A cell behaviour.

MCF10A cells grown in Matrigel make and organise a BM of laminin-332 and collagen-IV, whereas those grown in Alpha4 did not (Fig. 1C and D). To further interrogate the ability of MCF10A cells to make ECM, we examined the LC-MS/MS data specifically for components of the ECM expressed under each condition (Fig. 3B) [36]. 45 ECM components were identified in all three hydrogels with MCF10A cells encapsulated within them, including the chains of human laminin-332 (LAMA3, LAMB3), consistent with immunofluorescence (IF) data (c.f. Fig. 1C, D). However, the MCF10A cells in Matrigel showed a more diverse set of ECM proteins, with 19 proteins not identified in either Alpha4 dilution. The LC-MS/MS data from cells in Matrigel indicated collagen-IV chains, COL4A1 and COL4A2, required for correct BM organisation and assembly, as well as COL4A5, collagens 17 and 18, and three other human specific laminin isoforms. However, the sequence of human and mouse collagen IV isoforms are virtually identical, so it is not possible to determine if these are being made by the MCF10A cells or if the cells are reorganising this from the Matrigel. These data indicate that Matrigel provides a more permissive environment for MCF10A cells to differentiate and organise an appropriate ECM than does Alpha4.

To determine the effect of softening Alpha4 on MCF10A cell function we undertook quantitative comparison of the LC-MS/MS data by analysing the mean fold-change and *P*-value for differentially identified proteins, examining total proteins and not just components of the Matrisome (Fig. 3C). Comparison between cells within stiff Alpha4 with those in Matrigel showed that more proteins were significantly downregulated in the SAPH than were upregulated. In contrast, similar numbers of proteins were significantly upregulated and downregulated in soft Alpha4 gels in comparison with Matrigel. When comparing the two Alpha4 hydrogel cultures, there were significantly more downregulated proteins in the stiffer culture conditions. Thus, MCF10A cells

show differential protein expression between the three conditions, but neither 50 % nor 75 % Alpha4 fully recapitulated Matrigel. Overall, these differences in protein expression between soft and stiff Alpha4 samples and Matrigel indicate that key aspects of Matrigel contribute to the MCF10A organoid phenotype.

Although Alpha4 diluted to 50 % appeared to be the most favourable SAPH condition for MCF10A function, the protein expression profile was still distinct from cells in Matrigel. To understand the functional significance of these differences, we undertook gene ontology over representation analysis on the LC-MS/MS data to determine what key biological processes were different between cells grown in 50 % Alpha4 and Matrigel. Using clusterProfiler's gene ontology overrepresentation test, we identified significantly upregulated processes (p < 0.05) enriched in soft Alpha4 gels in comparison with Matrigel (Fig. 3D). Biological processes found to be significantly enriched in soft Alpha4 relative to Matrigel included those involved in regulating catabolic enzyme activity. Proteins associated with the humoral immune and inflammatory responses were detected, although these did not constitute the most enriched biological processes upregulated in soft Alpha4 samples. Downregulated biological processes mostly appeared to be affiliated with metabolic and housekeeping processes. These findings suggested that key difference in MCF10A cell behaviour in soft Alpha4 compared to Matrigel is a reduction in metabolic activity.

These data suggest that reducing the stiffness of Alpha4 improves viability and growth of MEC clusters, but that the mechanics alone are not sufficient to recapitulate the differentiation and organisation of cells in Matrigel.

3.4. MCF10A cells require laminin within the hydrogel scaffold to maintain acinar organisation

It was clear from the preceding data that MCF10A cells required specific biochemical signals from components of Matrigel that were not provided by a synthetic SAPH. SAPH such as Alpha4 have no specific functional motifs that would interact with cell surface receptors such as integrins. Previous studies have shown that MECs form polarised acini within laminin containing hydrogels [8]. Furthermore, these allowed primary MECs to produce milk proteins in response to the lactogenic hormone, prolactin. We therefore asked whether MCF10A acini would maintain their organisation if embedded into ECM based hydrogels of either laminin or collagen I. To initially test the response to collagen I and laminin we grew MCF10A cells within 4.5 mg/mL Matrigel for seven days so that they had formed multicellular acini with an established BM (c.f. Fig. 4A and Fig. 1). Live, intact acini were then extracted from the Matrigel and embedded within secondary hydrogels, either Matrigel, Alpha4, 1.5 mg/mL collagen-I or 6.1 mg/mL laminin-111. The concentrations of collagen-I and laminin-111 were chosen as these were able to form mechanically stable hydrogels capable of supporting cell cultures for at least seven days. Whereas acini in Matrigel and Alpha4 maintained their gross structure, those in collagen-I rapidly lost any

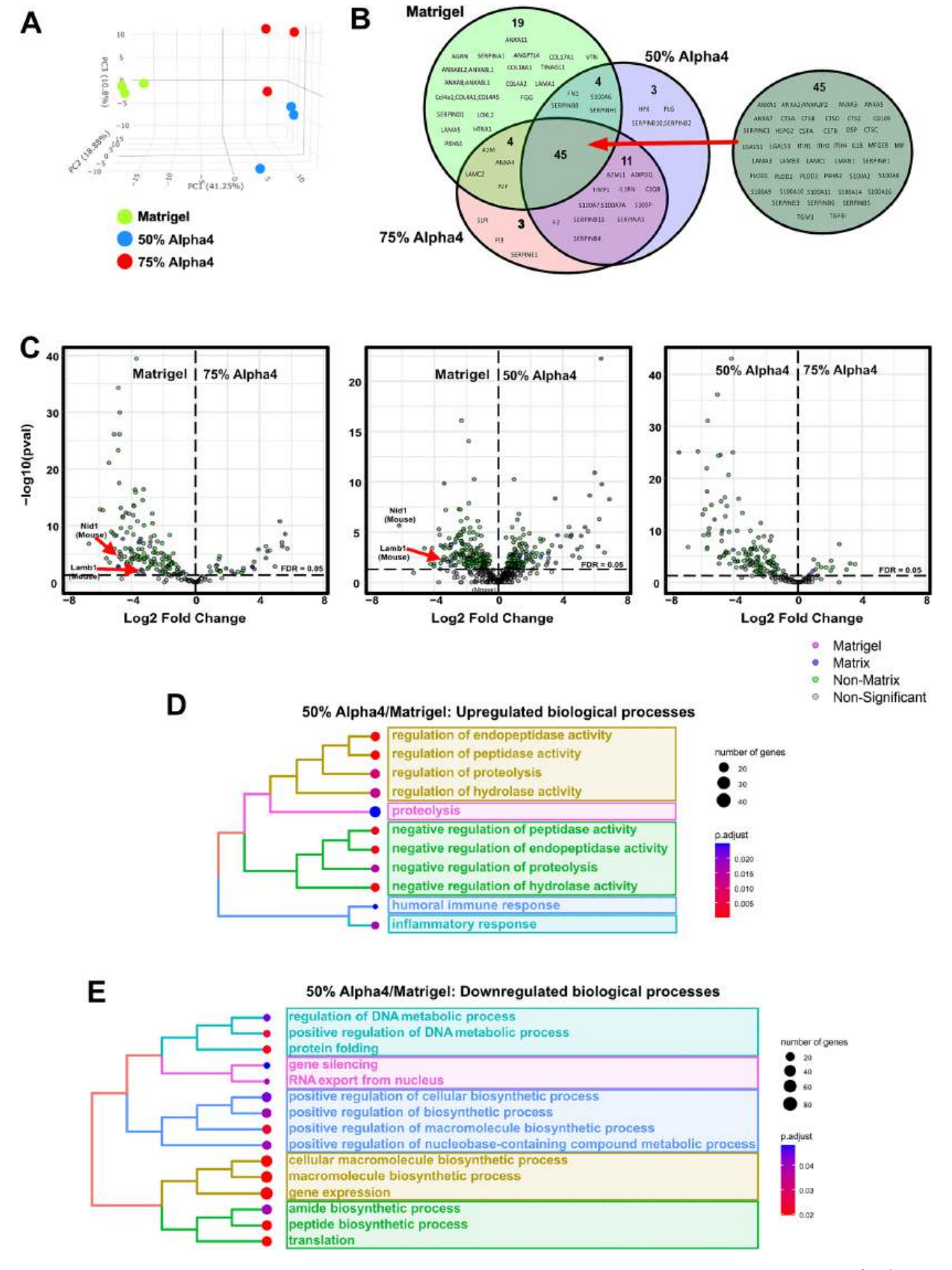


Fig. 3. Mass spectrometry analysis of MCF10A cells encapsulated in Matrigel, stiff and soft Alpha4 identifies distinct proteomic profiles.

A. Principal component analysis of proteomic analysis from of proteins quantified in cell-laden Matrigel, soft (50 %) and medium (75 %) Alpha4 gels. Three replicates from each condition were analysed.

- B. Venn diagram of mass spectrometry analysis showing unique and overlapping Matrisome proteins from each condition.
- C. Volcano scatter plot showing mass spectrometry comparison of proteins isolated from MCF10A organoids cultured in Matrigel, 75 % Alpha4 and 50 % Alpha4 hydrogels. Statistical significance ($-\log 10~p$ -value) is shown versus magnitude of change (Log2 Fold Change). Plots depict upregulated (positive ratio) and down-regulated (negative ratio) proteins. A positive Log2 change indicates proteins enriched in the condition named in the right hand panel of each plot. P-value calculated via MSqRob from three independent replicates (p < 0.05). Matrigel specific proteins (mouse) are indicated, along with matrisome (Matrix) and other (Non-Matrix) proteins.
- D. Gene set enrichment analysis (GSEA) comparing MCF10A organoids grown in Matrigel with those grown in soft (50 %) Alpha4, filtered for GO: biological processes. Indicates pathways that are upregulated in MCF10A cells encapsulated in 50 % Alpha 4 relative to Matrigel.
- E. GSEA as in D but identifying pathways that are downregulated in MCF10A cells encapsulated in Alpha4 relative to Matrigel.

organisation and cells became dispersed. In contrast, MCF10A acini in laminin hydrogels maintained a clearly defined organisation.

To determine whether laminin-111 hydrogels were able to provide signals for acinar development, single MCF10A cells were encapsulated in laminin-111 gels and compared to cells in Matrigel. Cells were imaged over 21 days using brightfield and confocal IF imaging. Brightfield imaging showed acini forming in laminin-111 gels that were similar to those in Matrigel over the same time frame (Fig. 4B). To measure organoids within the Matrigel and laminin, cultures were fixed and stained with DAPI on days 7, 14 and 21 days. Fluorescent images of organoids were then counted in QuPath (Fig. 4C). Overall, fewer organoids were growing within the laminin gels compared to Matrigel. The total number of organoids decreased over the 21-day period in both gels. We quantified the size and circularity of the organoids. There was little difference in acini between the Matrigel and laminin cultures (Fig. 4C). Acini grew in size in both Matrigel and laminin between days 7 and 14. No significant difference in circularity was found between Matrigel and laminin 111 cultures. Any minor differences might be explained by the more complex composition of Matrigel regarding growth factors, although the laminin-111 used was purified from Matrigel.

We encapsulated single MCF10A cells in either 4.5 mg/mL Matrigel or 6.1 mg/mL laminin-111 for 7, 12 and 21 days. Acini were then extracted, fixed and immunostained for human laminin-332, cleaved caspase-3, β -catenin and collagen-IV (Fig. 4D). Acini from laminin-111 hydrogels were indistinguishable from those in Matrigel and displayed a clearly defined BM, seen through both laminin-332 and collagen-IV localisation. β -catenin showed clearly defined cell-cell junctions, and cleaved caspase-3 positive cells indicated apoptosis occurring within the central lumen of the developing structures. The similarity of MCF10A acini in laminin-111 compared to Matrigel indicate that it alone can provide the appropriate biochemical and mechanical cues for MEC culture.

3.5. Laminin functionalises SAPHs to support MCF10A acinar development

Laminin-111 provided an appropriate biochemical and biomechanical microenvironment to support MCF10A cells organisation into the same polarised, acinar structures as seen in Matrigel. However, purified laminin is mechanically soft and requires a high concentration to form a hydrogel, making it impractical as a 3D culture scaffold [35]. We therefore asked if supplementing SAPHs such as Alpha4 with lower concentrations of laminin would combine both the required mechanics and a suitable biochemical signal. We therefore encapsulated single MCF10A cells within either Matrigel, laminin-111, Alpha4 or Alpha4 supplemented with 1 mg/mL laminin-111. We also included a comparison with Alpha4 diluted with Matrigel at a final concentration of 1.5 mg/mL. Cultures were maintained for seven days before imaging (Fig. 5A). MCF10A cells formed organoids as previously seen within Matrigel, laminin-111 and Alpha4. Including 1.5 mg/mL Matrigel within Alpha4 gel promoted acinar development, although the structures appeared confined to discrete areas within the hydrogel, suggesting that Matrigel and Alpha4 do not fully mix. Notably, addition of laminin to Alpha4 did not stimulate acinar development in MCF10A cells. Furthermore, when Alpha4 was combined with laminin a precipitate was seen to form, suggesting that they were not fully compatible. A possible clue as to why Alpha4-laminin hydrogels contained a precipitate is that Alpha4 has an overall positive charge. We therefore asked if the soft, negatively charged SAPH, Alpha7, would be compatible with laminin. We encapsulated MCF10A cells for seven days within either Alpha7 alone, Alpha7 with Matrigel or Alpha7 with 1 mg/mL laminin (Fig. 5B). MCF10a cells were viable in Alpha7 alone but appeared mostly to remain as single cells or very small clusters. In contrast, addition of either Matrigel or laminin increased the number of acinar-like structures formed over seven days. We asked what the effect on hydrogel stiffness was when combining laminin-111 with Alpha7. We used rheometry to measure the mechanics of undiluted Alpha7 with Alpah7 diluted with either PBS or 1 mg/mL laminin (Fig. 5C). Alpha7 was stiffer than Alpha4 (G' \sim 1200 Pa), but diluted with either laminin or PBS was considerably softer. Laminin containing Alpha7 was stiffer than that with PBS, at ~75

We compared the functionalisation of both Alpha4 and Alpha7 with Matrigel or laminin by encapsulating single MCF10A cells into each hydrogel or composite and culturing them for seven days. Acini were then isolated, fixed, and immunostained for human laminin-332, cleaved caspase-3, collagen-IV and β -catenin (Fig. 5D). Compared with Matrigel alone, Alpha4 did not support correct organisation of MCF10A acini when supplemented with laminin, although supplementing with Matrigel did. Alpha7 alone was unable to support acinar organisation, and MCF10A cells were seen as very small cell clusters with no BM deposition. However, Alpha7 supplemented with laminin promoted acini that were indistinguishable from those in Matrigel. Indeed, these acini showed clear BM organisation with both laminin-332 and collagen-IV, identical to that of cells cultured in Matrigel.

To determine how laminin altered the behaviour of MCF10A cells within Alpha7 we performed an unbiased proteomic analysis. Triplicate cultures of MCF10A cells were encapsulated within either Alpha7 or Alpha7 supplemented with 1 mg/mL laminin-111 for 14 days. To eliminate proteins within the culture media and the laminin-111 we also analysed cell-free preparations of each scaffold, with any proteins with the same abundance in both blank and cell-containing samples removed from downstream analysis. Over 2000 proteins were detected by LC-MS/ MS from each sample from both the Alpha7 and Alpha7/laminin. After normalisation of peptide intensity, principal component analysis clearly separated lysates obtained from Alpha7 and Alpha7/laminin gels (Fig. 6A). As expected from the dramatic difference in acinar organisation (Fig. 5C and D), this clearly shows that supplementing laminin-111 to Alpha7 changes protein expression in MCF10A cells. Quantitative comparison of the LC-MS/MS data for significant changes in protein expression indicated broad differences in protein expression between the Alpha7 and Alpha7/laminin cultures (Fig. 6B). In order to identify differentially regulated biological processes regulated by laminin we used clusterProfiler's gene ontology overrepresentation test. This identified numerous significantly upregulated processes (p < 0.05) when laminin was added to Alpha7 (Fig. 6C). In contrast to Alpha4 hydrogels, these included processes associated with epithelial cell differentiation,

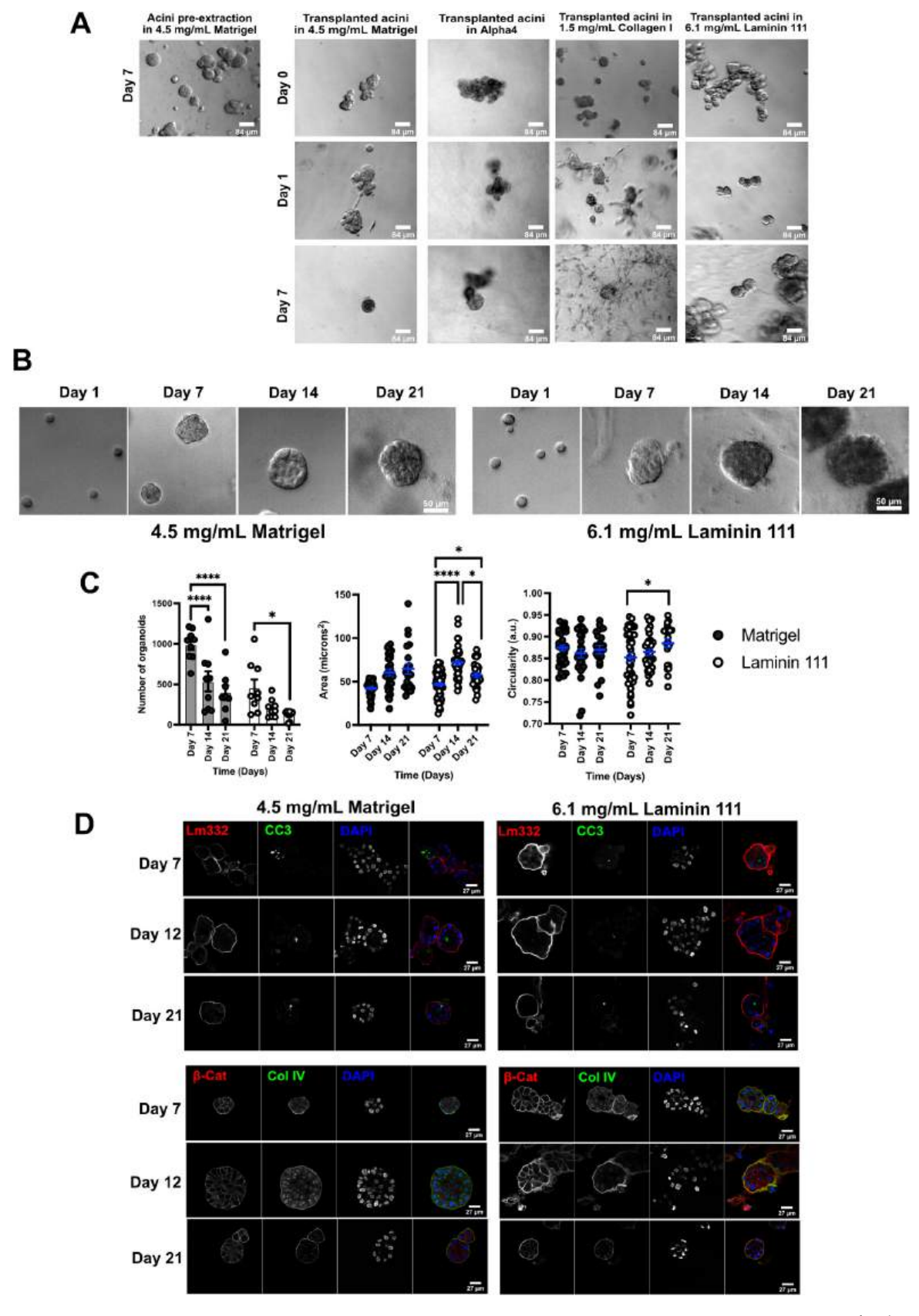


Fig. 4. MCF10A acinar development and polarity requires laminin.

A. MCF10A organoids initially grown in 4.5 mg/mL Matrigel for 7 days before being isolated and transplanted into either Matrigel, Alpha4, 1.5 mg/mL collagen-I or 6.1 mg/mL laminin-111. Brightfield images of the transplanted organoids at the indicated times. Scale bar = 84 µm.

- B. Representative brightfield images of single cell suspensions of MCF10A cells embedded in either 4.5 mg/mL Matrigel or 6.1 mg/mL laminin-111 and cultured for 1, 7, 14 and 21 days. Scale bar $= 50 \mu m$.
- C. Quantification of organoid number, size and circularity of MCF10A cells grown in either Matrigel or laminin-111 for the indicated number of days. All measurements were performed at least 3 times. Data = mean \pm SD. P-value: * <0.05; *** <0.001; **** <0.0001.
- D. MCF10A organoids grown in either 4.5 mg/mL Matrigel or 6.1 mg/mL laminin-111 for the indicated number of days. Organoids were extracted from the 3D cultures and immunostained. Left panel: laminin-332 (Lm332) and cleaved caspase-3 (CC3). Right panel: β -catenin (β -Cat) and collagen-IV (Col IV). Nuclei were stained with DAPI (scale bars, 27 μ m).

development and processes expected if MCF10A cells were displaying a phenotype indicative of MEC differentiation. Downregulated biological processes included DNA replication, mRNA processing, and mitosis. This is consistent with the smaller size and lack of BM organisation of cell clusters in Alpha7, overall suggesting that MCF10A cells are less proliferative in this hydrogel in the absence of laminin (Fig. 6D).

Together, these data show that optimisation of SAPHs as a mechanical scaffold along with appropriate supplemental microenvironmental components such as tissue specific ECM proteins allows for a reproducible alternative to Matrigel for MEC culture models.

4. Discussion

In this study we have demonstrated that SAPHs Alpha4 and Alpha7 support the viability of mammary epithelial cells in 3D culture models. However, the properties of these hydrogels need optimisation to replace established culture conditions using organic matrices like Matrigel. SAPHs provide biocompatible and chemically defined hydrogel scaffolds which are extremely consistent between batches. Different peptides, however, have widely different properties, including their charge and mechanical stiffness. The results presented here show that cell type specific optimisation of SAPHs is important to fully utilise them in 3D tissue culture models.

Previous studies found a neutrally charged SAPH was compatible with MCF7 and MDA-MB-231 breast cancer models, recapitulating features such as tumour hypoxia and drug accessibility [24]. In contrast, neutrally charged SAPHs did not support MCF10A cell viability or organoid growth (data not shown), whereas charged peptides such as Alpha4 did. However, although MCF10A cells were viable and proliferated within Alpha4, they failed to recapitulate the organoid polarisation seen in Matrigel. One aspect of SAPHs determined by their peptide sequence is mechanical stiffness. Alpha 4 and Alpha5, another positively charged SAPH of higher mechanical stiffness, have been shown to support kidney epithelial organoid development, including a laminin basement membrane [25]. In that study, the stiffer Alpha5 better supported more nephron like cells, including mature podocytes. Differentiation into appropriate cell types in kidney organoids did not require specific functionalisation of the SAPHs with motifs or ECM components. MECs and breast cancer cells have been shown to respond significantly to ECM stiffness [9,33]. Matrigel is both significantly softer than SAPHs and inconsistent between batches, although other studies have measured values within the same range as our data presented here [35]. We found Matrigel to have G' of ~6 Pa, and this could be stiffened using an interpenetrating alginate network to \sim 170 Pa. Other studies that have used Matrigel-alginate networks have reported values for G' between 30 and 310 Pa using the same CaSO₄ concentrations [14]. Our measurements for Alpha4 and Alpha7 are consistent with values reported by the manufacturer. The stiffness of SAPHs can be tuned through the amphiphilicity of the sequence altering the interactions between fibres. Utilising different SAPH sequences revealed that pancreatic cancer cells showed reduced apoptosis within a stiff hydrogel (Pepti-Gel® Alpha2, G' ~ 10 kPa) compared to a softer one (PeptiGel® Gamma2, G' ~ 4 kPa) [20]. We were able to modify the stiffness of Alpha4 and Alpha7 by diluting them in an aqueous buffer. This had the effect of reproducibly softening the SAPHs, avoiding the necessity for

different peptide sequences and corresponding changes in charge. The G' of Alpha4 could be reduced approximately 2.5-fold before the network became unstable. Proteomic analysis demonstrated that MCF10A cells within Alpha4 hydrogels synthesised epithelial specific ECM components, including collagen IV and laminin. However, although softening Alpha4 did alter gene expression in MECs, this alone did not recapitulate the protein expression or polarisation seen with organoids grown in Matrigel. Overall, this suggests that key biochemical signals are required to form an organised BM.

Laminin-111, the major component of Matrigel, can promote primary MEC differentiation in 3D cultures [37]. High concentration purified laminin-111 formed hydrogels which promoted 3D acinar polarisation of MCF10A cells. We were able to combine laminin at lower concentrations within SAPHs, but this was then only compatible with negatively charged Alpha7. Laminin appeared to precipitate within Alpha4 and failed to support MEC acinar organisation. One possible explanation is that laminin compatibility is mediated by electrostatic interactions with the charged SAPH. Electrostatic interactions between cells and their environment regulate viability, differentiation, and adhesion. Positively charged SAPHs promote cell attachment via interactions between negative charges on the cell surface and the positively charged scaffold [38-40]. Conversely, negatively charged hydrogels can repel negatively charged cell surface moieties, resulting in cells remaining single and rounded, as we observed in nonfunctionalised Alpha7 [39]. Electrostatic interactions between oppositely charged moieties are involved in laminin binding, where anionic glycans presented on dystroglycan [41,42] form salt bridges with cationic lysine residues within the laminin globular domains [43]. These interactions drive laminin polymerisation and BM formation [44-46]. Thus, the peptide sequence of SAPHs may be critical for how macromolecules such as laminin interact within the hydrogel, and how they are presented to cells to provide key functionality. Consideration of the individual properties of SAPHs would appear to be essential for successful functionalisation.

A SAPH based on Alpha7 and functionalised with laminin recapitulated the MCF10A acinar organisation seen in complete Matrigel. Proteomic analysis indicated differentiation of MCF10A cells, with upregulation of BM components, as well as regulators of MEC differentiation such as Stat6 and interferon regulatory factor 6 [23,47]. Pathway enrichment analysis highlighted several biological processes that were upregulated that indicate mammary morphogenesis. One limitation in our study is we have only analysed MCF10A cells, a cell line. Although these do show a clear epithelial phenotype, they do differ in some respects from primary MECs, most notably in that they do not express hormone receptors. These limitations of MCF10A cells have been well characterised [48]. Overall, these results show that SAPHs can be functionalised for MEC culture, creating a scaffold that is defined, simple and modifiable. Although here we used purified laminin, a fully synthetic functionalised hydrogel could be achieved by using recombinant full-length laminin or laminin fragments.

CRediT authorship contribution statement

Eliana Lingard: Data curation, Investigation, Writing – original draft, Writing – review & editing. **Siyuan Dong:** Investigation. **Anna**

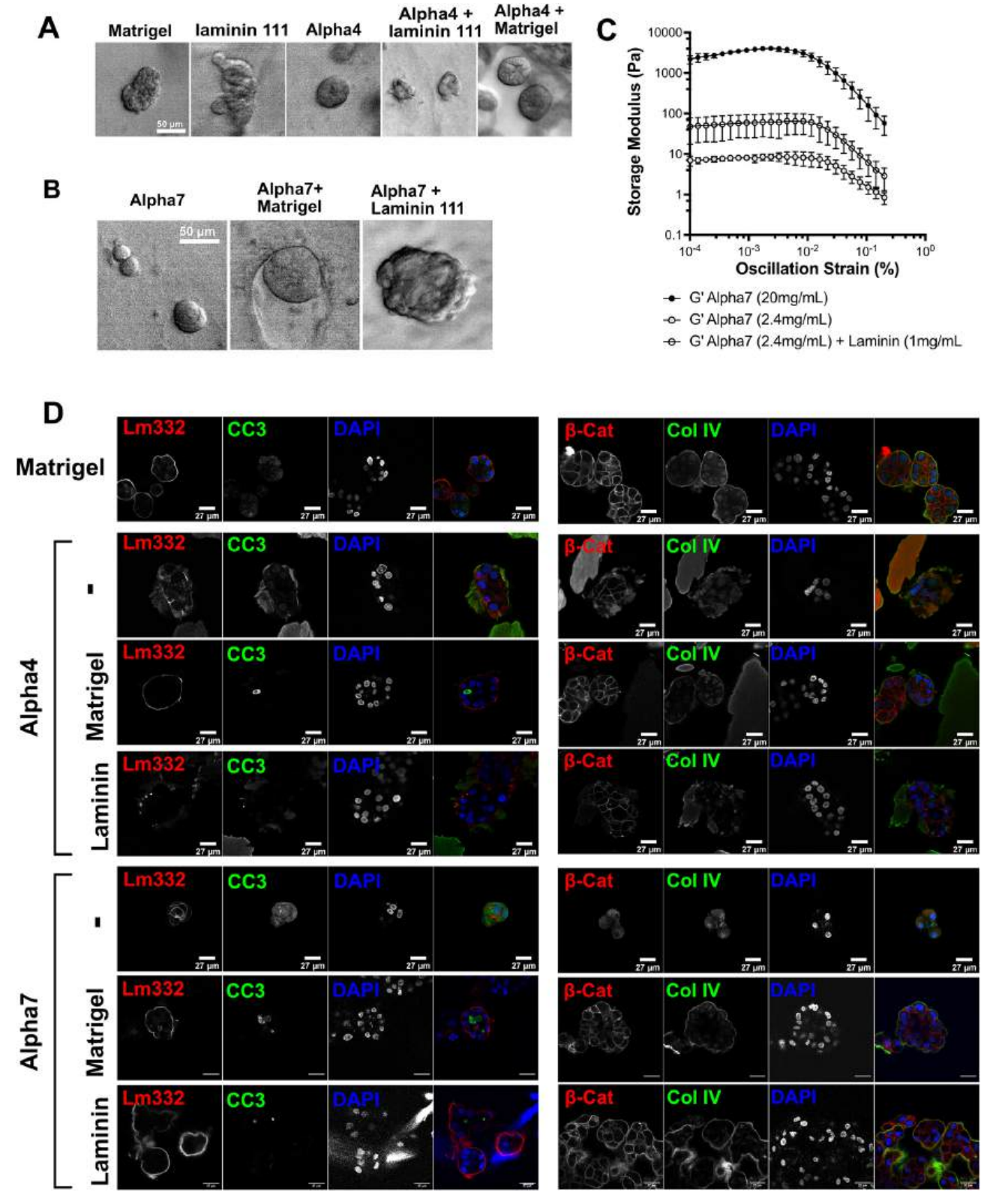


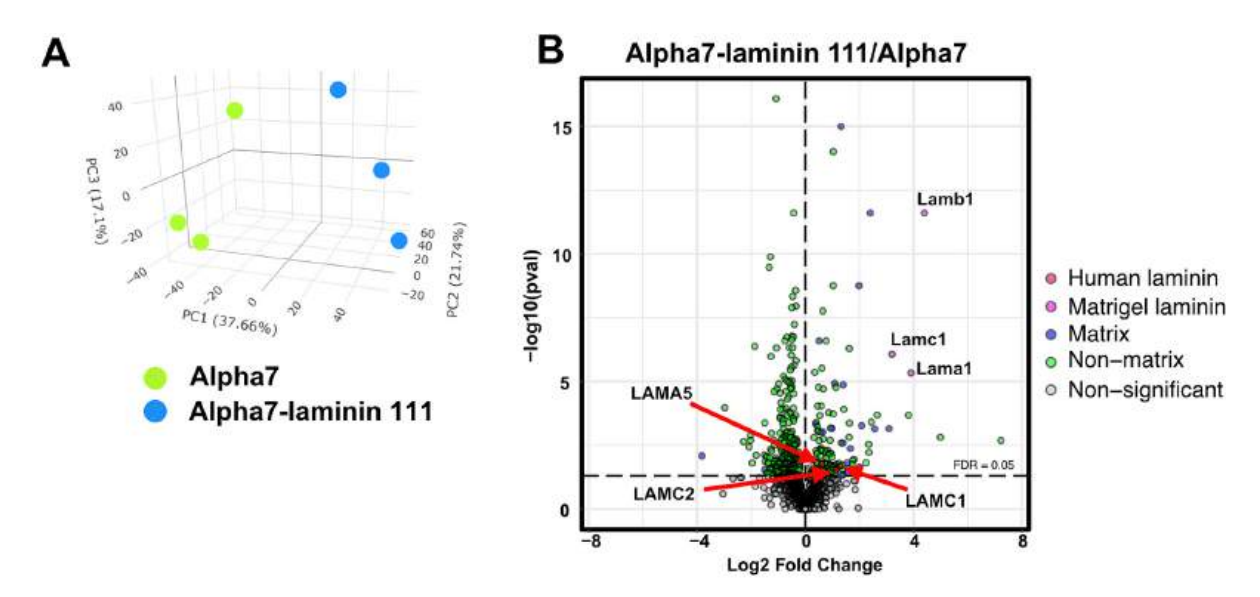
Fig. 5. SAPHs functionalised with laminin support MCF10A cell acinar development.

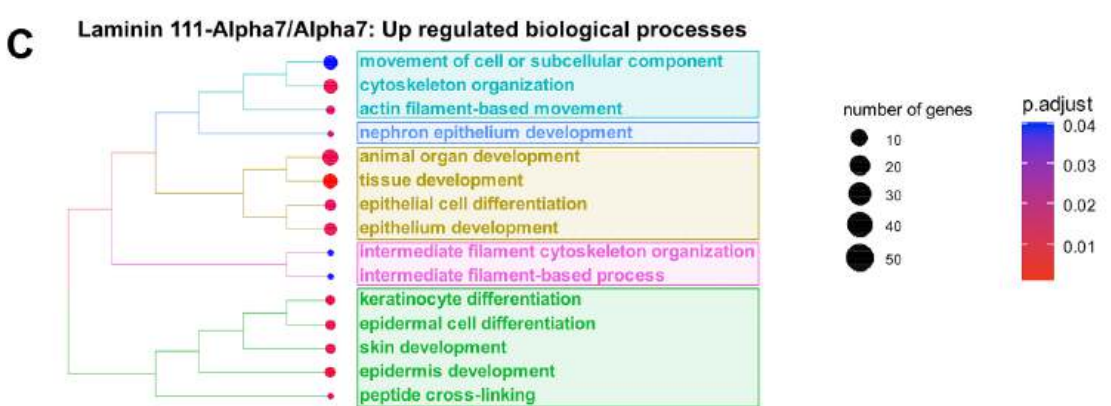
A. Comparison of MCF10A organoids grown for 7 days from single cell suspensions in Matrigel, laminin-111, Alpha4, or Alpha4 supplemented with either Matrigel or laminin-111. Brightfield images show lack of organoids in Alpha4 gels combined with laminin. Scale bar $= 84 \mu m$.

B. MCF10A organoids grown from 7 days in Alpha7 alone or supplemented with Matrigel or laminin-111. Scale bar = 84 µm.

C. Oscillatory rheometry comparison of storage (G') modulus of Alpha7, and Alpha7 diluted with either laminin-111 or PBS. All measurements were performed at least 3 times. Means \pm SD are shown.

D. MCF10A organoids grown in either Matrigel, Alpha4 or Alpha7. Alpha4 and Alpha 7 were supplemented with either laminin-111 or Matrigel as indicated. Organoids were cultured for 7 days, extracted from the 3D cultures and immunostained. Left panel: laminin-332 (Lm332) and cleaved caspase-3 (CC3). Right panel: β -catenin (β -Cat) and collagen-IV (Col IV). Nuclei were stained with DAPI. Scale bars = 27 μ m.





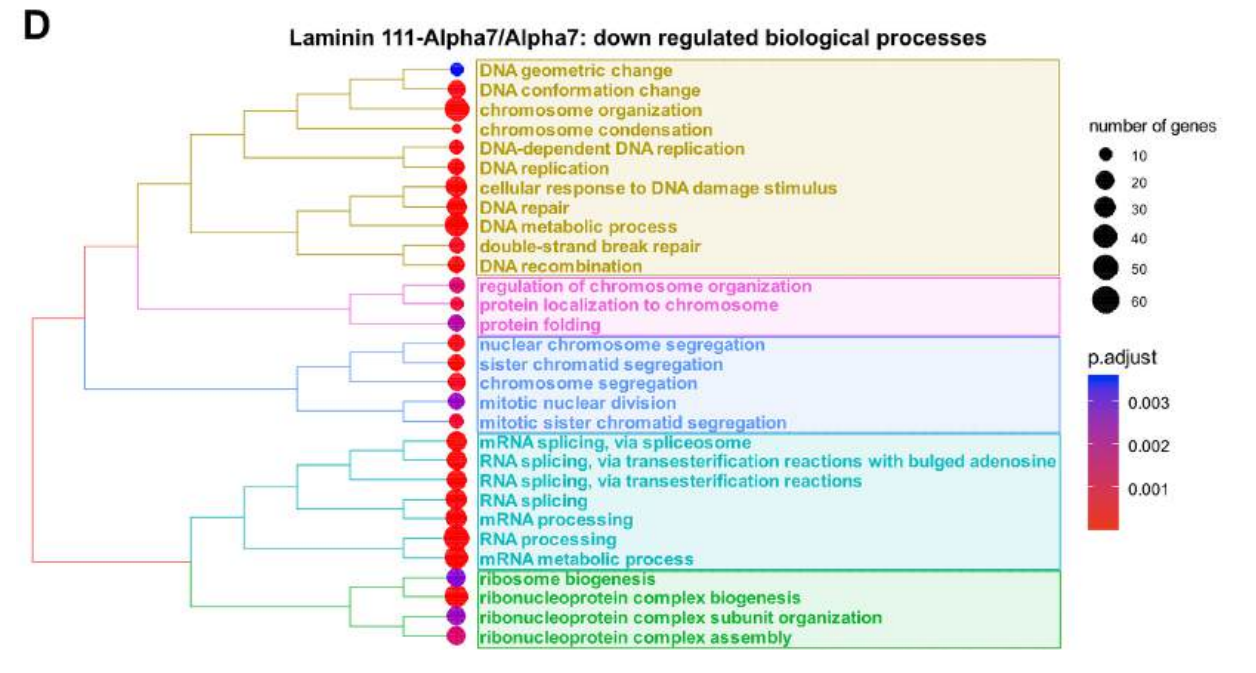


Fig. 6. Mass spectrometry analysis of MCF10A organoids grown in Alpha7 with laminin show protein expression indicating MEC differentiation.

MCF10A organoids were grown for 7 days in either Alpha7 hydrogels or Alpha7 supplemented with laminin-111. Proteins were isolated and quantified by mass spectrometry. Three independent replicates were analysed.

A. Principal component analysis of organoids grown in Alpha7 and Alpha7 supplemented with laminin show separation between the two conditions.

B. Volcano scatter plot showing mass spectrometry comparison of proteins isolated from MCF10A organoids in Alpha7/laminin hydrogels versus Alpha7 hydrogels. Statistical significance ($-\log 10 \ p$ -value) is shown versus magnitude of change (Log2 Fold Change). Plots depict upregulated (positive ratio) and downregulated (negative ratio) proteins. A positive Log2 change indicates protein abundance is enriched in the Alpha7-Laminin111 condition. *P*-values calculated using MSqRob from three independent replicates (p < 0.05). Mouse laminin (Lama1, Lamb1 Lamc1, from Matrigel) are indicated. Human laminin isoforms identified (LAMA5, LAMC1, LAMC2) show increased abundance in Alpha7/laminin hydrogels versus Alpha7 hydrogels.

C. Gene set enrichment analysis (GSEA) conducted on the data in B. showing GO:biological processes upregulated in MCF10A cells in Alpha7/laminin hydrogels versus Alpha7 hydrogels. Key process include various terms associated with epithelial differentiation.

D. GSEA conducted on the data in B. showing GO:biological processes downregulated in MCF10A cells in Alpha7/laminin hydrogels versus Alpha7 hydrogels. Relationships between groups are displayed by connecting lines.

Hoyle: Data curation, Investigation. Ellen Appleton: Data curation. Alis Hales: Data curation, Investigation. Eldhose Skaria: Data curation, Investigation. Craig Lawless: Formal analysis. Isobel Taylor-Hearn: Formal analysis. Simon Saadati: Formal analysis. Qixun Chu: Investigation. Aline F. Miller: Funding acquisition. Marco Domingos: Conceptualization, Funding acquisition, Project administration, Writing – review & editing. Alberto Saiani: Project administration, Writing – review & editing, Conceptualization, Funding acquisition. Joe Swift: Conceptualization, Funding acquisition, Project administration, Writing – review & editing. Andrew P. Gilmore: Conceptualization, Funding acquisition, Project administration, Supervision, Writing – original draft, Writing – review & editing.

Declaration of competing interest

Manchester Biogel in part funded this research through a PhD studentship to the lead author (EL).

Aline Miller and Alberto Saiani were shareholders, directors, and consultants for Manchester Biogel.

Data availability

Proteomics data have been deposited to the ProteomeXchange Consortium via the PRIDE partner repository [49] with the identifier PXD045193.

Acknowledgements

The project was funded through the UK Regenerative Medicine Platform (UKRMP) grant "Acellular/Smart Materials – 3D Architecture" (MR/R015651/1). EL was supported by a PhD scholarship from The University of Manchester, sponsored by UKRMP and Manchester Bio-GEL. AH was supported by a studentship from the Biotechnology and Biological Sciences Research Council (BBSRC). EA and I.T-H were supported by studentships from the Wellcome Trust. JS was supported by a BBSRC David Phillips Fellowship (BB/L024551/1). ES and the Wellcome Trust Centre for Cell-Matrix Research were funded by the Wellcome Trust (088785/Z/09/Z). Proteomics was performed by the Biological Mass Spectrometry Core Facility (supported by BBSRC, the Wellcome Trust and the University of Manchester Strategic Fund). This work was supported in part by the International Alliance for Cancer Early Detection, an alliance between Cancer Research UK, Canary Center at Stanford University, the University of Cambridge, OHSU Knight Cancer Institute, University College London and the University of Manchester. Work in the Royce Institute is funded through EP/ R00661X/1, EP/S019367/1, EP/P025021/1 and EP/P025498/1.

Statement of significance

3-dimensional (3D) organoid cultures are an important tool in cell biology. 3D organoids models have been particularly important in understanding the biology of the mammary gland, as mammary epithelial

cells (MECs) will form functional organoids in 3D culture conditions. However, mammary gland organoid models have largely relied on a reconstituted basement membrane (BM) extract, Matrigel. Matrigel has many limitations, including: biochemical complexity; significant batch to batch variation; xenogenic properties; and poor mechanical properties. These limitations have prompted development of cell scaffolds that offer more consistency, definition and tuneability, such as polyethyleneglycol (PEG) or polyacrylamide (PAM), but often these have limitations such as biocompatibility for 3D culture. Self-assembling peptide hydrogels (SAPHs) are a class of promising synthetic scaffolds for 3D culture. SAPHs are short, synthetic, amphipathic peptides that self-assemble into fibrillar structures which entangle with each other, forming hydrated, fibrillar scaffolds. Here we show that optimising the SAPH along with appropriate biochemical signals allows correct differentiation and gene expression in 3D MEC cultures.

References

- K.M. Yamada, E. Cukierman, Modeling tissue morphogenesis and cancer in 3D, Cell 130 (4) (2007) 601–610.
- [2] P. Barros da Silva, et al., Reshaping in vitro models of breast tissue: integration of stromal and parenchymal compartments in 3D printed hydrogels, Front. Bioeng. Biotechnol. 8 (2020) 494.
- [3] S.J. Bidarra, et al., A 3D in vitro model to explore the inter-conversion between epithelial and mesenchymal states during EMT and its reversion, Sci. Rep. 6 (1) (2016) 27072.
- [4] C. Ligorio, et al., Graphene oxide containing self-assembling peptide hybrid hydrogels as a potential 3D injectable cell delivery platform for intervertebral disc repair applications, Acta Biomater. 92 (2019) 92–103.
- [5] A.C. Luca, et al., Impact of the 3D microenvironment on phenotype, gene expression, and EGFR inhibition of colorectal cancer cell lines, PLoS One 8 (3) (2013) e59689.
- [6] E.A. Aisenbrey, W.L. Murphy, Synthetic alternatives to matrigel, Nat. Rev. Mater. 5 (7) (2020) 539–551.
- [7] R.W. Orkin, et al., A murine tumor producing a matrix of basement membrane, J. Exp. Med. 145 (1) (1977) 204–220.
- [8] J. Aggeler, et al., Cytodifferentiation of mouse mammary epithelial cells cultured on a reconstituted basement membrane reveals striking similarities to development in vivo, J. Cell Sci. 99 (1991) 407–417.
- [9] M.L. Li, et al., Influence of a reconstituted basement membrane and its components on casein gene expression and secretion in mouse mammary epithelial cells, Proc. Natl. Acad. Sci. USA 84 (1) (1987) 136–140.
- [10] C.S. Hughes, L.M. Postovit, G.A. Lajoie, Matrigel: a complex protein mixture
- required for optimal growth of cell culture, Proteomics 10 (9) (2010) 1886–1890.

 [11] N.C. Talbot, T.J. Caperna, Proteome array identification of bioactive soluble proteins/peptides in matrigel: relevance to stem cell responses, Cytotechnology 67 (5) (2015) 873–883.
- [12] T.A. Prokhorova, et al., Teratoma formation by human embryonic stem cells is site dependent and enhanced by the presence of matrigel, Stem Cells Dev. 18 (1) (2008) 47-54
- [13] S.S. Soofi, et al., The elastic modulus of Matrigel™ as determined by atomic force microscopy, J. Struct. Biol. 167 (3) (2009) 216–219.
- [14] O. Chaudhuri, et al., Extracellular matrix stiffness and composition jointly regulate the induction of malignant phenotypes in mammary epithelium, Nat. Mater. 13 (2014) 970.
- [15] H. Liu, et al., Removal of lactate dehydrogenase-elevating virus from human-in-mouse breast tumor xenografts by cell-sorting, J. Virol. Methods 173 (2) (2011) 266–270.
- [16] B. Díaz-Bello, et al., Method for the direct fabrication of polyacrylamide hydrogels with controlled stiffness in polystyrene multiwell plates for mechanobiology assays, ACS Biomater. Sci. Eng. 5 (9) (2019) 4219–4227.

- [17] C.R. Below, et al., A microenvironment-inspired synthetic three-dimensional model for pancreatic ductal adenocarcinoma organoids, Nat. Mater. 21 (1) (2022) 110-119
- [18] J. Gao, et al., Controlling self-assembling peptide hydrogel properties through network topology, Biomacromolecules 18 (3) (2017) 826–834.
- [19] M.R. Caplan, et al., Control of self-assembling oligopeptide matrix formation through systematic variation of amino acid sequence, Biomaterials 23 (1) (2002) 219–227
- [20] D. Lachowski, et al., Self-assembling polypeptide hydrogels as a platform to recapitulate the tumor microenvironment, Cancers 13 (13) (2021).
- [21] A. Imere, et al., Engineering a cell-hydrogel-fibre composite to mimic the structure and function of the tendon synovial sheath, Acta Biomater. 119 (2021) 140–154.
- [22] B. Raphael, et al., 3D cell bioprinting of self-assembling peptide-based hydrogels, Mater. Lett. 190 (2017) 103–106.
- [23] L.A. Castillo Diaz, et al., Osteogenic differentiation of human mesenchymal stem cells promotes mineralization within a biodegradable peptide hydrogel, J. Tissue Eng. 7 (2016) 2041731416649789.
- [24] H.C. Clough, et al., Neutrally charged self-assembling peptide hydrogel recapitulates in vitro mechanisms of breast cancer progression, Mater. Sci. Eng. C 127 (2021) 112200.
- [25] N.J. Treacy, et al., Growth and differentiation of human induced pluripotent stem cell (hiPSC)-derived kidney organoids using fully synthetic peptide hydrogels, Bioact. Mater. 21 (2022) 142–156.
- [26] S. Tyanova, T. Temu, J. Cox, The MaxQuant computational platform for mass spectrometry-based shotgun proteomics, Nat. Protoc. 11 (12) (2016) 2301–2319.
- [27] C. UniProt, UniProt: the universal protein knowledgebase in 2021, Nucleic Acids Res. 49 (D1) (2021) D480–D489.
- [28] L.E. Goeminne, K. Gevaert, L. Clement, Peptide-level robust ridge regression improves estimation, sensitivity, and specificity in data-dependent quantitative label-free shotgun proteomics, Mol. Cell. Proteomics 15 (2) (2016) 657–668.
- [29] T. Wu, et al., clusterProfiler 4.0: a universal enrichment tool for interpreting omics data, Innovation 2 (3) (2021) 100141.
- [30] G. Yu, Q.-Y. He, ReactomePA: an R/Bioconductor package for reactome pathway analysis and visualization, Mol. BioSyst. 12 (2) (2016) 477–479.
- [31] J. Debnath, S.K. Muthuswamy, J.S. Brugge, Morphogenesis and oncogenesis of MCF-10A mammary epithelial acini grown in three-dimensional basement membrane cultures, Methods 30 (3) (2003) 256–268.
- [32] S. Walker, et al., Oncogenic activation of FAK drives apoptosis suppression in a 3D-culture model of breast cancer initiation, Oncotarget 7 (43) (2016) 70336–70352.
- [33] K.R. Levental, et al., Matrix crosslinking forces tumor progression by enhancing integrin signaling, Cell 139 (5) (2009) 891–906.

- [34] P.P. Provenzano, et al., Matrix density-induced mechanoregulation of breast cell phenotype, signaling and gene expression through a FAK–ERK linkage, Oncogene 28 (2009) 4326.
- [35] F. Millesi, et al., Systematic comparison of commercial hydrogels revealed that a synergy of laminin and strain-stiffening promotes directed migration of neural cells, ACS Appl. Mater. Interfaces 15 (10) (2023) 12678–12695.
- [36] A. Naba, et al., The matrisome: in silico definition and in vivo characterization by proteomics of normal and tumor extracellular matrices, Mol. Cell. Proteomics 11 (4) (2012). M111 014647.
- [37] C.H. Streuli, et al., Laminin mediates tissue-specific gene expression in mammary epithelia, J. Cell Biol. 129 (3) (1995) 591–603.
- [38] M. Ferrari, F. Cirisano, M.C. Morán, Mammalian cell behavior on hydrophobic substrates: influence of surface properties, Colloids Interfaces 3 (2) (2019).
- [39] A. Nagayasu, et al., Efficacy of self-assembled hydrogels composed of positively or negatively charged peptides as scaffolds for cell culture, J. Biomater. Appl. 26 (6) (2010) 651–665.
- [40] G.B. Schneider, et al., The effect of hydrogel charge density on cell attachment, Biomaterials 25 (15) (2004) 3023–3028.
- [41] A. Faroni, et al., Self-assembling peptide hydrogel matrices improve the neurotrophic potential of human adipose-derived stem cells, Adv. Healthc. Mater. 8 (17) (2019) 1900410.
- [42] M.L. Weir, et al., Dystroglycan loss disrupts polarity and beta-casein induction in mammary epithelial cells by perturbing laminin anchoring, J. Cell Sci. 119 (Pt 19) (2006) 4047–4058.
- [43] T. Yoshida-Moriguchi, et al., O-mannosyl phosphorylation of alpha-dystroglycan is required for laminin binding, Science (New York, N.Y.) 327 (5961) (2010) 88–92.
- [44] H. Colognato, D.A. Winkelmann, P.D. Yurchenco, Laminin polymerization induces a receptor-cytoskeleton network, J. Cell Biol. 145 (3) (1999) 619–631.
- [45] E. Freire, T. Coelho-Sampaio, Self-assembly of laminin induced by acidic pH, J. Biol. Chem. 275 (2) (2000) 817–822.
- [46] S. Li, et al., Laminin-sulfatide binding initiates basement membrane assembly and enables receptor signaling in Schwann cells and fibroblasts, J. Cell Biol. 169 (1) (2005) 179–189.
- [47] K.A. Burgess, et al., Functionalised peptide hydrogel for the delivery of cardiac progenitor cells, Mater. Sci. Eng. C 119 (2021) 111539.
- [48] Y. Qu, et al., Evaluation of MCF10A as a reliable model for normal human mammary epithelial cells, PLoS One 10 (7) (2015) e0131285.
- [49] Y. Perez-Riverol, et al., The PRIDE database resources in 2022: a hub for mass spectrometry-based proteomics evidences, Nucleic Acids Res. 50 (D1) (2022) D543–D552.